

Element free formulation for connecting sub-domains modeled by finite elements

Chan-Ping Pan[†]

Department of Construction Engineering, National Taiwan University of Science and Technology, Taiwan

Hsing-Chih Tsai[‡]

Ecological and Hazard Mitigation Engineering Research Center, National Taiwan University of Science and Technology, Taiwan

(Received August 23, 2005, Accepted September 13, 2006)

Abstract. Two methods were developed for analyzing problems with two adjacent sub-domains modeled by different kinds of elements in finite element method. Each sub-domain can be defined independently without the consideration of equivalent division with common nodes used for the interface. These two methods employ an individual interface to accomplish the compatibility. The MLSA method uses the moving least square approximation which is the basic formulation for Element Free Galerkin Method to formulate the interface. The displacement field assumed by this method does not pass through nodes on the common boundary. Therefore, nodes can be chosen freely for this method. The results show that the MLSA method has better approximation than traditional methods.

Keywords: compatibility; sub-domain; element free; moving least square; finite element; beam; plane stress.

1. Introduction

A common problem in Finite Element analysis is defining a methodology to connect different domains together. One case of this problem is the use of dissimilar meshes of the same element type to model jointed sub-domains. A second case is the conjunction within a model of different element types. Both situations require that compatibility be maintained between jointed areas. Moreover, another focus in recent years has been the minimization of human effort spent to maintain such compatibilities.

The simplest and easiest way to maintain a compatible interface between sub-domains is to define and use the same node set. However, doing this will produce limitations on the automatic procedure, which causes element distortion. Therefore, some methods employ independent descriptions of displacements for sub-domains to be jointed together. These methods can be divided into the following six categories:

[†] Associate Professor, E-mail: pan.c.p@yahoo.com.tw

[‡] Post Doc., Corresponding author, E-mail: tsaihsingchih@gmail.com

1. Penalty method (Arora *et al.* 1991, Carey *et al.* 1982). A penalty spring is employed in the penalty method to minimize nodal displacement differences at adjacent boundaries. One major drawback to this approach is that the accuracy of approximation varies significantly based on the penalty springs stiffness selected. Therefore, the spring constant value should be studied and selected carefully.
2. Lagrange multiplier method (Rixen *et al.* 1998, Farhat and Geradin 1992, Chang *et al.* 1987, Houslyby *et al.* 2000). In the Lagrange multiplier method, both nodal displacements and Lagrange parameters are treated as independent variables. One major drawback of this method is that the order of stiffness matrix increases due to the use of independent Lagrange parameters. Also, the ordinary procedure for Gauss elimination needs to be modified to add those Lagrange parameters to unknowns.
3. Transition elements for jointed areas (Dohrmann and Key 1999, Liao *et al.* 1998). Transition elements were developed to link together two or more regions. The connected regions could be modeled using various elements or meshes. Meticulous care in developing and selecting transition elements is essential. Furthermore, such elements can almost never be used in a model other than for which it was specifically designed. The number of nodes used for the interface is also limited by transition elements used.
4. Master-slave concept (Quiroz and Beckers 1995, Dohrmann and Key 2000, Dohrmann *et al.* 2000). The basic idea underlying the master-slave concept is the replacement of the slave boundary geometric definition with that of the master boundary to ensure displacement's continuity. The major restriction of this model is that standard practice requires the master boundary to have fewer nodes than those of the slave boundary. The simulated flexibility of the interface is restricted by the master boundary, which is more rigid than that of the slave.
5. Equal work concept (Shim *et al.* 2002, McCune *et al.* 2000). Multi-point constraint equations can be formulated by equating the work done on both sides of an interface. Thus, a relationship among nodal degrees of freedoms can be provided between regions.
6. Independent common boundary method (pseudo-node method) (Aminpour *et al.* 1995). Unlike the use of the displacement description on the master side in the master-slave concept, this method creates an independent description of the displacement field, where residuals exist on both sides of a common boundary. Although the displacements of other points on the adjacent boundaries do not match with the displacements on the common boundary, differences can be minimized through mesh refinement. The assumed displacement field on the common boundary can be either a single polynomial function or piecewise polynomial function defined by several independent nodes. Those on the common boundary replace the unknowns of displacement on adjacent boundaries (Lancaster and Salkauskas 1981, Gordon and Wixson 1978).

Several existed ways can be used to define a common boundary of different finite elements. Two methods were developed in the present paper: the collocation method and the MLSA method. The MLSA formulation for the displacement field of the common boundary has never been used before. The MLSA method uses a single polynomial function with continuously varied coefficients to simulate a common boundary. Compared with the collocation method, an infinite number of piecewise polynomial functions are used in the MLSA method. The assumed displacement field is based on a formulation, which is similar to the element free formulation (Belytschko *et al.* 1994, Ginman 1997, Nayroles *et al.* 1992), and the number and distribution of nodes on the common boundary can be chosen freely. Therefore, the same formulation can easily improve upon the quality

of the assumed displacement. The flexibility of this method is demonstrated through example given in the following.

The emphasis of this paper is on situations where a common boundary exists between different element types. The beam element and plane stress element are chosen to model the two sub-domains in order to illustrate the proposed methods. The detailed derivation of the two methods will be shown in the next section. The efficiency of these two methods is compared through an illustration of problems for which analytical solutions have been obtained through the application of beam theory.

The common boundary of the same element with dissimilar meshes were studied and analyzed by the authors in a separate paper (Tsai and Pan 2004).

2. Derivation of the two methods

The investigated issue in this paper is how to deal with a finite element model which contains both beam and plane stress elements having a common boundary. Several possibilities for the interface at the common boundary include the end point of the beam, or the entire side face of the beam, or the bottom (top) side of the beam. In each case, the analytical processes required are totally different. For this paper, only the common boundary in the bottom (top) side was investigated (Fig. 1).

The displacement fields assumed by each element are also different. The traditional beam element assumes a third degree polynomial for the transverse displacement (perpendicular to the beam axis), and a linear polynomial for the axial displacement (parallel to the beam axis). The displacement field assumed by the plane stress element is dependent upon the shape functions. Use of 9-nodes Lagrange shape functions assumes that both the transverse and axial displacements are the 2nd-degree polynomial in the master element. Therefore, polynomial differs for these two elements in terms of degree. In addition to the displacement fields assumed for each element, a third and independent displacement field is assumed in the two methods discussed here. According to the compatibility requirement, displacements at the common boundary must be the same. Thus, in theory, all of three displacement fields should be equal.

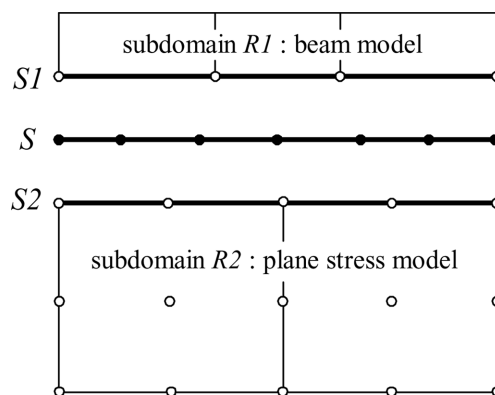


Fig. 1 Three boundaries used to model the interface

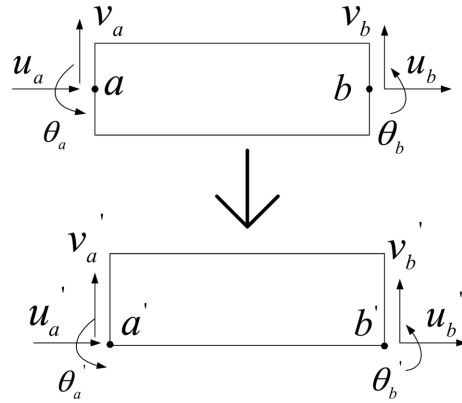


Fig. 2 Transformation of degrees of freedom for a beam element

However, the beam elements in the investigated problems are constantly subject to the internal contact forces transmitted across the interface by plane stress elements. For the described problem generally an analytical solution does not exist. The assumed displacement field can approximate a precise solution only by increasing the element number. The compatibility of these methods is achieved by an approximation procedure, which is controlled by the mesh refinement.

Three displacement fields are assumed on the interface. The first is assumed for the beam element boundary, the second is assumed for the plane stress element boundary, and the third is assumed for the common boundary. For convenience in working with these different boundaries, the beam element boundary was named as $S1$, and the plane stress element boundary as $S2$, and the common boundary as S (Fig. 1). The elements adjacent to the common boundary are defined as: sub-domain $R1$ for beam elements and sub-domain $R2$ for plane stress elements.

The stiffness matrix of the beam element is formulated for the six nodal displacements of the neutral axis of the beam section. However, the compatibility requirement should be satisfied to interface displacements at the bottom (top) face of the beam section. For the beam element under study it is essential to transfer the degree of displacement freedom on the neutral axis $\{q_b\}$ to the degree of freedom on the interface $\{q'_b\}$ (Fig. 2).

$$\{q_b\} = \{u_a \ v_a \ \theta_a \ u_b \ v_b \ \theta_b\}^T \quad (1)$$

$$\{q'_b\} = \{u'_a \ v'_a \ \theta'_a \ u'_b \ v'_b \ \theta'_b\}^T \quad (2)$$

$$\{q_b\} = [T_b]\{q'_b\} \quad (3)$$

$$[T_b] = \begin{bmatrix} 1 & 0 & -h/2 & 0 & 0 & 0 \\ 0 & 1 & 0 & 0 & 0 & 0 \\ 0 & 0 & 1 & 0 & 0 & 0 \\ 0 & 0 & 0 & 1 & 0 & -h/2 \\ 0 & 0 & 0 & 0 & 1 & 0 \\ 0 & 0 & 0 & 0 & 0 & 1 \end{bmatrix} \quad (4)$$

The stiffness matrix of beam element formulated for the degree of freedom on the adjacent boundary $[k'_b]$ can be obtained from the transformation matrix $[T_b]$ and the original stiffness matrix $[k_b]$ as follows:

$$[k'_b] = [T_b]^T [k_b] [T_b] \quad (5)$$

where $[k_b]$ is the original stiffness matrix of a beam element incorporating the six degrees of freedom on the neutral axis.

There are two transitional degrees of freedom and one rotational degree of freedom for the nodes used in beam elements and only two transitional degrees of freedom for the nodes used in plane stress elements. Therefore, it is necessary only to transfer the two transitional degrees of freedom to the common boundary (u and v in Eq. (2)).

Two transitional degrees of freedom per node exist on the common boundary. The general assumption for displacement field on the common boundary is:

$$\{s\} = \{s^u \ s^v\}^T = [N(\xi)] \{q_{si}\} \quad (6)$$

$$[N] = \begin{bmatrix} N^u \\ N^v \end{bmatrix} = \begin{bmatrix} N_1 & 0 & N_2 & 0 & \dots & N_m & 0 \\ 0 & N_1 & 0 & N_2 & \dots & 0 & N_m \end{bmatrix} \quad (7)$$

$$\{q_{si}\} = \{u_1 \ v_1 \ u_2 \ v_2 \ \dots \ u_m \ v_m\}^T \quad (8)$$

In the above equations, $[N]$ is a $2*m$ matrix containing the shape functions corresponding to the local coordinate, ξ , of the common boundary S . $\{q_{si}\}$ is a vector of $2*m$ generalized displacements associated with the m nodes chosen on the common boundary. The vector $\{s\}$ has two transitional displacements which represent the transverse and axial displacements $\{s^u\}$ and $\{s^v\}$ of any point along the common boundary.

2.1 Collocation method

The elements and nodes are derived independently for the adjacent sub-domains. In order to connect these sub-domains, proper procedures must be followed to ensure compatibility and force transmission across these adjacent boundaries. Displacements are determined by the shape functions of the individual model on each side. The element types used in examples are the beam element with shear deformation taken into account and the 9-nodes Lagrange plane stress element. In order to improve accuracy, a single 4th-degree polynomial function, defined by five nodal displacements, is assumed to form the third and independent displacement field of the common boundary, S , in the Eq. (6). This means that the size of the vector $\{q_{si}\}$, which includes two sets of five degrees of freedom, is equal to ten. Every transitional degree of freedom on adjacent boundaries will impact upon the value of the degree of freedom for the five nodes along the common boundary.

The potential energy of an element on the adjacent boundary is calculated from either the sub-domain $R1$ of the beam model or the sub-domain $R2$ of the plane stress model. The relevant equation is:

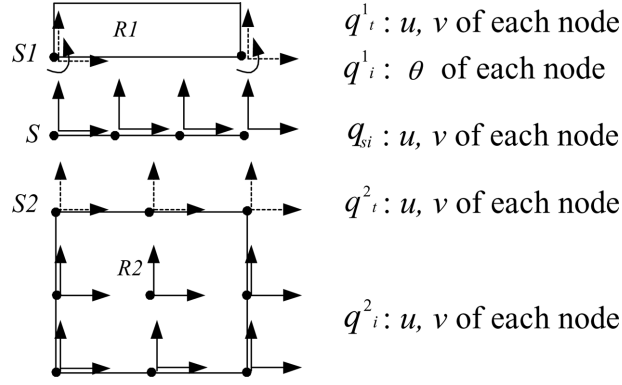


Fig. 3 q_i^1 and q_i^2 transferred to q_{si}

$$\Pi^j = \frac{1}{2} \{q^{ji} \ q^{jt}\} [k^j] \begin{Bmatrix} q^{ji} \\ q^{jt} \end{Bmatrix} - \{q^{ji} \ q^{jt}\} \begin{Bmatrix} f^{ji} \\ f^{jt} \end{Bmatrix} \tag{9}$$

There are two cases of the upper index j in above equation. $j = 1$ denotes an element in the beam model and $j = 2$ denotes an element in the plane stress model. The lower index i indicates the degree of freedom of nodes along the adjacent boundary and the lower index t indicates the degree of freedom for nodes along the adjacent boundary that need to be transferred to the ones on the common boundary (Fig. 3). $\{q\}$ represents the displacement vector associated with these two sets of nodes. While $[k^j]$ represents the element stiffness matrix and $\{f\}$ represents the force vector.

The degree of freedom on the adjacent boundaries for both beam and plane stress models are obtained using Eq. (6). The local coordinate of each node is calculated through linear interpolation.

$$\begin{Bmatrix} q^{ji} \\ q^{jt} \end{Bmatrix} = [T^j] \begin{Bmatrix} q^{ji} \\ q_{si} \end{Bmatrix} \tag{10}$$

$\{q_{si}\}$ is a vector with ten degrees of freedom for the five nodes chosen along the common boundary. $[T_j]$ represents a transformation matrix.

Inserting Eq. (10) into Eq. (9), the potential energy of a neighboring element may be expressed as follows:

$$\Pi^j = \frac{1}{2} \{q^{ji} \ q_{si}\} [k_i] \begin{Bmatrix} q^{ji} \\ q_{si} \end{Bmatrix} - \{q^{ji} \ q_{si}\} \begin{Bmatrix} f^{ji} \\ f_t \end{Bmatrix} \tag{11}$$

After the transformation, the corresponding stiffness matrix and force vector of an element can be represented by the following equations:

$$[k_i] = [T^j]^T [k^j] [T^j] \tag{12}$$

$$\{f_i\} = [T^j]^T \{f^j\} \tag{13}$$

Along adjacent boundaries, only the nodal displacements are consistent with the simulation of a

common boundary. It means that discrepancies between these three displacement fields can be expected. However increasing the number of nodes can reduce discrepancies, so the compatibility requirement can be approximated during refinement procedures.

2.2 MLSA method

In order to get a more reliable approximation using the collocation method, either a higher polynomial degree or more divided sections must be used to simulate the common boundary. Otherwise, the moving least square approximation can be applied to any number of nodes within one section that is simulated using a fixed polynomial degree.

The displacement field of the common boundary S assumed by the MLSA method is as follows:

$$\{s\} = \{u \ v\}^T = \{s^u \ s^v\}^T \quad (14)$$

Two transitional degrees of freedom, u and v , are assumed for each node along the common boundary. Both u and v are formulated independently. Since the formulations are similar, only a representative value, s^d , is used in the following equations. The upper index, d , could be either u or v , depending on which was focused as the displacement item. In the MLSA method the displacement s^d can be expressed as:

$$s^d = \sum_{j=1}^n b_j(\xi) a_j(\xi) \equiv \{b\}^T \{a\} \quad (15)$$

where n is defined as the degree of the selected polynomial function plus one, and $\{b\}$ represents a vector of n polynomial bases. While $\{a\}$ represents a vector of n polynomial coefficients. The value of s^d is calculated by using the relative local coordinate ξ of a point on S . Notice that both $\{b\}$ and $\{a\}$ are functions of the local coordinate ξ . In the present study, a 2nd-degree polynomial (quadratic polynomial) is chosen, by assuming the value of n equal to three. The vector $\{b\}$ has three polynomial bases and $\{a\}$ contains three unknown coefficients, represented by a_i . Therefore:

$$\{b\}^T = \{1 \ \xi \ \xi^2\} \quad (16)$$

$$\{a\}^T = \{a_0(\xi) \ a_1(\xi) \ a_2(\xi)\} \quad (17)$$

A scalar J is defined as the weighted sum of squared residuals, with the residual being the difference between the approximated displacement s^d and the nodal displacement q_{si}^d along a common boundary:

$$J = \sum_{i=1}^m w(\xi - \xi_i) (b^T a - q_{si}^d)^2 \quad (18)$$

where m represents the number of nodes defined along a common boundary. While w is a weighting function, which is defined by s^d and q_{si}^d . The matrix form of J is derived through the following equation:

$$J = ([B]^T \{a\} - \{q_{si}\})^T [W] ([B]^T \{a\} - \{q_{si}\}) \quad (19)$$

$$\{q_{si}^d\} = \{q_1^d \ q_2^d \ \dots \ q_m^d\}^T \quad (20)$$

$\{q_{si}^d\}$ represents a vector of m nodal displacements and $[B]$ is a $n*m$ matrix composed of m vectors $\{b\}$ where ξ_i represents the local coordinate for node i . $[W]$ represents an $m*m$ matrix. The diagonal components of $[W]$ are weighting functions evaluated at each node. These two matrices assume the form:

$$[B] = [b(\xi_1) \ b(\xi_2) \ \dots \ b(\xi_m)] \quad (21)$$

$$[W] = \begin{bmatrix} w(\xi - \xi_1) & 0 & \dots & 0 \\ 0 & w(\xi - \xi_2) & \dots & 0 \\ \vdots & \vdots & \ddots & \vdots \\ 0 & 0 & \dots & w(\xi - \xi_m) \end{bmatrix} \quad (22)$$

In the above equations, $\xi_1, \xi_2, \dots, \xi_m$, are used to denote the local coordinates of m nodes.

A modified exponential weighting function is adopted in this analysis. The weighting function is shown as follows:

$$w_I(d_I^{2k}) = \begin{cases} \frac{e^{-(d_I/c)^{2k}} - e^{-(d_{mI}/c)^{2k}}}{1 - e^{-(d_{mI}/c)^{2k}}} & d_I \leq d_{mI} \\ 0 & d_I > d_{mI} \end{cases} \quad (23)$$

d_I is used to denote the distance between the considered point ξ and the nodal point coordinate ξ_i while c represents a constant parameter to control the shape of the weighting function, the value of which can be determined by calculating the sequential value of d_I . In order to involve enough nodes to evaluate the unknown coefficients, c should be larger than the $(m-1)$ th smaller value d_I . k represents a constant related to the order of required differentiation. The value of k is set as one in this paper. d_{mI} determines the range of influence of a particular node, and can be obtained by p times c . Increasing the value of d_{mI} can smooth out the displacement field s^d . The requirement of d_{mI} is that the number of nodes must be greater than n .

The unknown coefficients a_i can be determined by setting J to be a minimum value, the so-called "moving least square approximation".

$$\frac{\partial J}{\partial a} = [H]\{a\} - [G]\{q_{si}^d\} = 0 \quad (24)$$

In the above equation, the terms $[H]$, $[G]$ and $\{a\}$ are obtained as:

$$[H] = [B][W][B]^T \quad (25)$$

$$[G] = [B][W] \quad (26)$$

$$\{a\} = [H]^{-1}[G]\{q_{si}^d\} \quad (27)$$

The displacement field of a common boundary can be expressed as the derived displacement vector $\{a\}$.

$$s^d = \{b\}^T [H]^{-1} [G] \{q_{si}^d\} \quad (28)$$

By substituting Eq. (28) in Eq. (6), the shape function $[N^d]$ can be recognized to be:

$$[N^d] = \{b\}^T [H]^{-1} [G] \quad (29)$$

Following the same procedure used in section 2, the representation of the common and adjacent boundaries can be obtained. The vector size of $\{q_{si}\}$ in Eq. (8) is $(m^u + m^v)$, with m^u being the number of nodal points chosen for u and m^v being the number of nodal points chosen for v . The vector $\{q_{si}\}$ comprises two sets of degrees of freedom chosen independently for u and v . However, as the values of m^u and m^v are usually the same, $[N]$ is a $2*2n$ matrix.

The displacement vector $\{q_{si}\}$ of the common boundary can be chosen either from one or both sides of adjacent boundaries. None of the chosen nodes should share a common position to avoid numerical problems. From the observation of the above equations it is evident that the weighting function is the key aspect of this method. Some function parameters will be examined later in this paper.

After the basic unknowns $\{q_{si}\}$ have been solved, the displacements at those nodes should be interpreted as s^d obtained by Eq. (28) instead of using $\{q_{si}^d\}$ directly.

However, an ill condition might occur when the number of nodes is greater than the one on the adjacent boundaries, while forecasting no one wants to use less than three nodes to formulate a quadratic polynomial. A suggestion of choosing the number of nodes in the common boundary will be made in the example problem.

3. Results and comparisons

Slender beams with a T- or rectangular section can be simulated using beam elements or through a model comprising beam elements for flange and plane stress elements for web. Therefore, such problems were chosen as illustrative examples due to the simplicity of getting an analytical solution from the beam model. Comparisons of these two methods will be shown through two illustrative examples in this section. In order to evaluate the displacement error between adjacent boundaries, an error norm is defined as follows:

$$ES^d = \frac{\int |d_{S1} - d_{S2}| dL}{d_{\max} L} \cdot 100\% \quad (30)$$

where d_{S1} and d_{S2} represent the displacement of sub-domain $S1$ and sub-domain $S2$ on the adjacent boundaries respectively, d_{\max} represents the maximum displacement of d_{S1} and d_{S2} . While L is used to denote the total length of a common boundary.

3.1 Simply supported beam problem

The problems illustrated in this study include: a simply supported rectangular beam (Fig. 4) and a

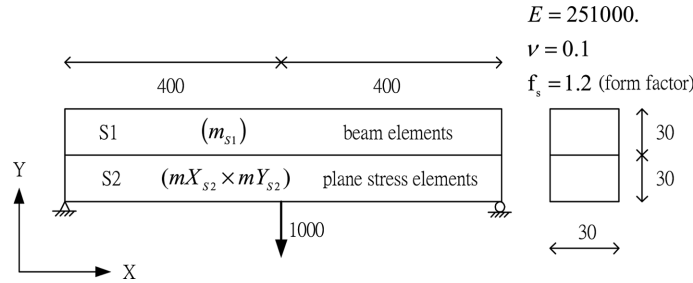


Fig. 4 Simply supported beam with rectangular cross section

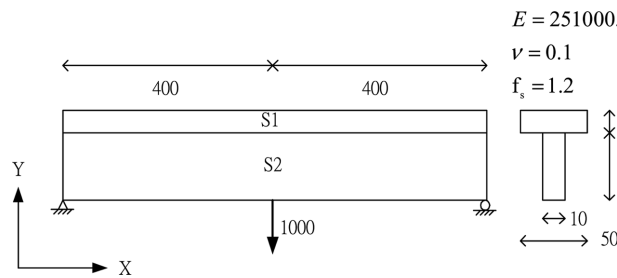


Fig. 5 Simply supported beam with T-shaped cross section

T-shaped beam (Fig. 5). Structural and loading data for these problems are shown in the figures. It is widely accepted that beam model displacement results are less flexible than those from plane stress models. However, as the length-to-depth ratio of the beam exceeds a value of 10, the theoretical results from these two models should be similar. The results derived from the beam model are used to compare results obtained in this paper. Shear deformation is included in beam theory calculations.

In the collocation method, five nodes with uniform spacing are used to simulate the common boundary. In the MLSA method, all nodes on adjacent boundaries are used to simulate the common boundary. $k = 1$ and $d_{ml} = 4c$ are defined as the default values for weighting function parameters. Four sets of meshes are used to simulate these two examples and the maximum displacement for each case was chosen to do the comparison.

m_{S1} represents the number of beam element used for the mesh while mX_{S2} and mY_{S2} stand for the numbers of plane stress elements used to divide X and Y directions, respectively.

Two factors have the potential to affect the calculated results. Because a coarse mesh model is stiffer than that of a fine mesh, numerical results value will increase through the refinement procedure. However, the compatibility condition is gradually attained through the increase in the number of elements. The gaps between adjacent boundaries are bigger for coarse mesh than those for fine mesh. Incompatible solutions make the structure more flexible than it should be, making the calculated results values to decrease through the refinement procedure. The calculated results are affected by these two opposing factors. Results in Table 1 and Table 2 show that the ratio of v_{max}/v_{ref} converges to one from the top (for instance, values of MLSA in Table 1 are 1.587 to 1.018) during the refinement procedure. This indicates that the incompatibility factor carries more importance than other factors in this illustrative example.

Calculated results will approach theoretical results from beam theory as expected. The results obtained by from using the collocation method (for example, ratio of v_{max}/v_{ref} is 0.996 for the finest

Table 1 Results of different methods for problems with rectangular section

Mesh	Collocation	MLSA	Collocation	MLSA	Collocation	MLSA
$(m_{S1}, mX_{S2}, mY_{S2})$	v_{max}/v_{ref}		ES^u		ES^v	
(2,3,1)	1.376	1.587	15.093%	30.842%	24.550%	13.998%
(4,6,1)	1.091	1.143	2.164%	6.908%	8.802%	8.404%
(8,12,1)	1.015	1.046	0.089%	2.398%	3.566%	3.492%
(16,24,2)	0.996	1.018	0.001%	1.100%	1.599%	1.587%

Table 2 Results of different methods for problems with T-shaped section

Mesh	Collocation	MLSA	Collocation	MLSA	Collocation	MLSA
$(m_{S1}, mX_{S2}, mY_{S2})$	v_{max}/v_{ref}		ES^u		ES^v	
(2,3,1)	1.267	1.409	15.731%	24.077%	25.142%	19.942%
(4,6,1)	1.085	1.135	3.223%	6.511%	8.848%	8.458%
(8,12,1)	1.018	1.046	0.585%	1.960%	3.561%	3.520%
(16,24,2)	1.003	1.022	0.133%	0.841%	1.594%	1.588%

mesh) are slightly better than those obtained by using the MLSA method (for example, ratio of v_{max}/v_{ref} is 1.018 for the finest mesh). Discrepancies associated with adjacent boundaries can be obtained from ES values, the results of which show the collocation method to return more accurate results for the value of ES^u (in Table 1, 0.001% vs. 1.100%). However, the MLSA method returns more accurate results for the value of ES^v (in Table 1, 1.599% vs. 1.587%). The v_{max}/v_{ref} ratios for both methods converge to one in both examples. While ES values converge to zero for both as well.

3.2 Problem characterized by relatively complicated displacement field

A simply supported beam subjected to four reverse point loadings was used as an example of a relatively complicated displacement field (Fig. 6). Two sets of meshes were chosen to test the two methods. Mesh definitions are designated by the three values m_{S1} , mX_{S2} , and mY_{S2} . Default parameters with the MLSA method were employed. The displacements along the line between two supports were selected for comparison.

By considering Fig. 7, it can be observed as the results from the collocation method differ significantly from the analytical results. The analytical solution shows two big waves, while the collocation method results show two straight lines. The possible reason may be the inability of the

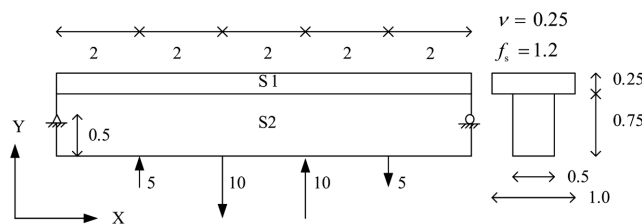


Fig. 6 Simply supported beam subjected to concentrated loadings

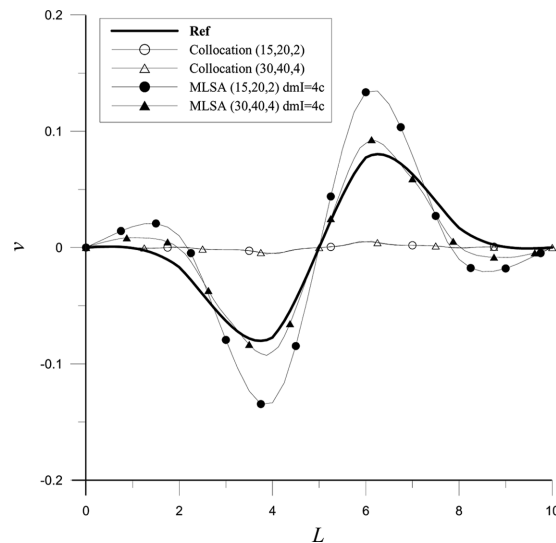


Fig. 7 Vertical displacement field (v) along the common boundary

assumed 4th-degree polynomial function to give an approximate solution for the current displacement field, since the polynomial degree used to simulate the common boundary in the collocation method is bounded by the number of nodes. The polynomial degree is always equal to the number of nodes minus one. In order to get a better approximation, more nodes are required to simulate this common boundary. Two procedures suggest themselves as possible approaches by which to improve the calculated results. The first is to use a polynomial with higher degrees. The second is to divide the common boundary by using a greater number of nodes. Extra derivation and programming efforts are required to accommodate these corrections. However, the MLSA method results approached the analytical results in the refinement procedure. A good method should be suitable for all kinds of problem, and the MLSA method can include any number of nodal points by the same derivation and the same program. Therefore, the MLSA method is suitable to simulate both simple and complicated displacement fields.

MLSA method convergence demonstrates that using a coarse mesh delivers results that are overly flexible due to incompatibility problems.

Two parameters used for the MLSA method are now discussed in detail. One is the influence range of each node, d_{ml} , and the other is the chosen nodes for the common boundary. Firstly, the three values of d_{ml} ($2c$, $4c$, $6c$ and $8c$) are used in the finer mesh. As shown in Fig. 8, the results of these three sets of d_{ml} are very similar, indicating that results are not sensitive to the value of d_{ml} . A smaller d_{ml} value can decrease the stiffness matrix bandwidth, thus decreasing calculation time. The lower bound of d_{ml} is suited to the illustrative example.

The arrangement of nodes along the common boundary is also tested for the same problem. The number and the distribution of nodes were changed to observe the effect on results. Seven different arrangements included five uniform distribution sets of nodes in number equal to: 5, 7, 11, 31, 81. The set of 31 nodes coincides with the distribution nodes of beam elements. The set of 81 nodes coincides with the distribution of plane stress elements. The other two sets of arrangement are non-uniform distribution (5, 101 nodes). The set of 101 nodes is the combination of nodes used for beam and plane stress elements. The non-uniform 5 nodes are arranged to close the location where

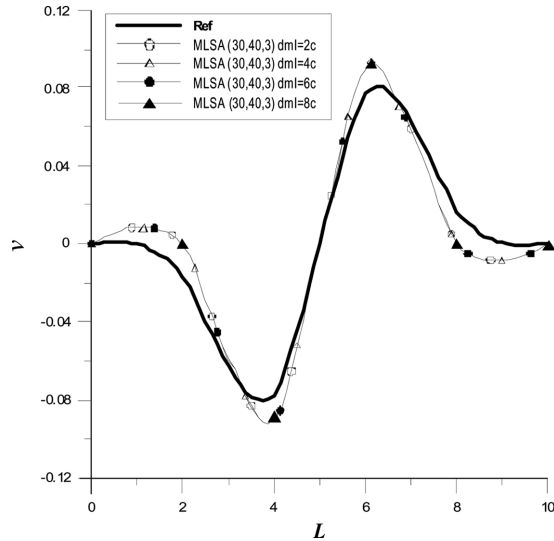


Fig. 8 Results obtained by different d_{ml} values

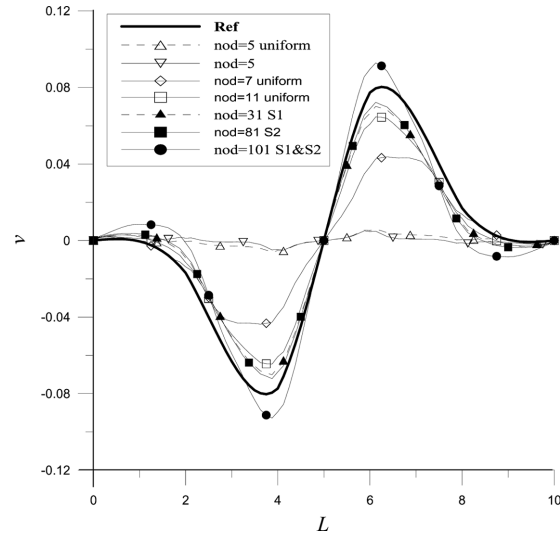


Fig. 9 Results obtained by different arrangement of nodes

the extreme values of the displacement field occur i.e. the nodal positions are $L = 0.0, 3.8, 5.0, 6.2, 10.0$. In Fig. 9, the results for 5 nodes show that moving the nodes to extreme positions is not useful. Calculated results show that convergence can rather be achieved by a small number of uniformly distributed nodes. The results provided by 11 uniformly distributed nodes are similar to those results achieved with 31 and 81 nodes. The simple choice of this illustrated example is to adapt all the nodes corresponding to elements on the adjacent boundaries.

From the results shown in this example, using the summation of nodes in adjacent boundaries (101 nodes) gives the best result. And, it is a simple choice for users. However, the results of 31 nodes are close to the results of 81 nodes. Therefore, the number of nodes has little effects in certain range. The users can chose a less number of nodes to get better numerical efficiency. The choice depends on the displacement shape of common boundary and the number of elements used in both regions. Only experienced users are suggested to make their own choices.

4. Conclusions

General methods used to connect different elements are presented in this paper. An independent displacement field is used to model the common boundary between the two sub-domains to be jointed together. In the present study, two methods are developed to build this displacement field: the collocation method and the MLSA method. The MLSA method is newly proposed in this study. The advantages of MLSA formulation include the ease of element mesh and free to choose node numbers and node positions in common boundary. Since the number of nodes can be chosen to be a smaller number than original nodes. Therefore, a smaller number of equations will result from this method. If the static condensation method is used to formulate the sub-domains, this advantage in numerical calculation will be even greater.

Two example problems are presented to compare the capability provided by these two methods.

Problems involving relatively simple displacement fields can be modeled well with either. The developed technique while problems with relatively complex displacement field cannot be modeled effectively using the collocation method; for such class of problems the MLSA method is the most appropriate. The major difference between the two methods is the possibility to vary the number of nodes used in the common boundary where can be easily varied in the MLSA method, making it a better choice.

References

- Aminpour, M.A., Ransom, J.B. and McCleary, S.L. (1995), "A coupled analysis method for structures with independently modeled finite element subdomains", *Int. J. Numer. Meth. Eng.*, **38**(21), 3695-3718.
- Arora, J.S., Chahande, A.I. and Paeng, J.K. (1991), "Multiplier methods for engineering optimization", *Int. J. Numer. Meth. Eng.*, **32**(7), 1485-1525.
- Belytschko, T., Lu, Y.Y. and Gu, L. (1994), "Element-free Galerkin methods", *Int. J. Numer. Meth. Eng.*, **37**(2), 229-256.
- Carey, G.F., Kabaila, A. and Utku, M. (1982), "On penalty methods for interelement constrains", *Comput. Meth. Appl. Mech. Eng.*, **30**(2), 151-171.
- Chang, T.Y., Saleeb, A.F. and Shyu, S.C. (1987), "Finite element solutions of two-dimensional contact problems based on a consistent mixed formulation", *Comput. Struct.*, **27**(4), 455-466.
- Dohrmann, C.R. and Key, S.W. (1999), "A transition element for uniform strain hexahedral and tetrahedral finite elements", *Int. J. Numer. Meth. Eng.*, **44**(12), 1933-1950.
- Dohrmann, C.R., Key, S.W. and Heinstein, M.W. (2000), "A method for connecting dissimilar finite element meshes in two dimensions", *Int. J. Numer. Meth. Eng.*, **48**(5), 655-678.
- Dohrmann, C.R., Key, S.W. and Heinstein, M.W. (2000), "Methods for connecting dissimilar three-dimensional finite element meshes", *Int. J. Numer. Meth. Eng.*, **47**(5), 1057-1080.
- Farhat, C. and Geradin, M. (1992), "Using a reduced number of Lagrange multipliers for assembling parallel incomplete field finite element approximations", *Comput. Meth. Appl. Mech. Eng.*, **97**(3), 333-354.
- Ginman, K.M.S. (1997), *Topology Optimization for 2-D Continuum Using Element Free Galerkin Method*, The University of Texas at Arlington.
- Gordon, W.J. and Wixson, J.A. (1978), "Shapard's method of metric interpolation to bivariate and multivariate data", *Mathematics of Computation*, **32**(141), 253-264.
- Houlsby, G.T., Liu, G. and Augarde, C.E. (2000), "A tying scheme for imposing displacement constraints in finite element analysis", *Communications in Numerical Methods in Engineering*, **16**(10), 721-732.
- Lancaster, P. and Salkauskas, K. (1981), "Surfaces generated by moving least square method", *Mathematics of Computation*, **37**(155), 141-158.
- Liao, C.L., Reddy, J.N. and Engelstad, S.P. (1998), "A solid-shell transition element for geometrically non-linear analysis of laminated composite structures", *Int. J. Numer. Meth. Eng.*, **26**(8), 1843-1854.
- McCune, R.W., Armstrong, C.G. and Robison, D.J. (2000), "Mixed-dimensional coupling in finite element models", *Int. J. Numer. Meth. Eng.*, **49**(6), 725-750.
- Nayroles, B., Touzot, G. and Villon, P. (1992), "Generalizing the finite element method diffuse approximation and diffuse element", *Computational Mechanics*, **10**(5), 307-318.
- Quiroz, L. and Beckers, P. (1995), "Non-conforming mesh gluing in the finite elements method", *Int. J. Numer. Meth. Eng.*, **38**(13), 2165-2184.
- Rixen, D., Farhat, C. and Geradin, M. (1998), "Two-step, two-field hybrid method for the static and dynamic analysis of substructure problems with conforming and non-conforming interface", *Comput. Meth. Appl. Mech. Eng.*, **154**(3-4), 229-264.
- Shim, K.W., Monaghan, D.J. and Armstrong, C.G. (2002), "Mixed dimensional coupling in finite element stress analysis", *Engineering with Computers*, **18**(3), 241-252.
- Tsai, H.C. and Pan, C.P. (2004), "Element free formulation used for connecting domain boundaries", *J. Chinese Ins. Eng.*, **27**(4), 585-596.